International Journal of Mass Spectrometry 290 (2010) 72–84

Contents lists available at ScienceDirect

International Journal of Mass Spectrometry

journal homepage: www.elsevier.com/locate/ijms

Laser desorption/ionization mass spectrometry on nanostructured semiconductor substrates: DIOS™ and QuickMass™

K.P. Law*

Centre for Analytical Bioscience, Laboratory of Biophysics, and Surface Analysis, School of Pharmacy, University of Nottingham, Nottingham, UK

ARTICLE INFO

Article history:
Received 24 September 2009
Received in revised form
22 November 2009
Accepted 3 December 2009
Available online 11 December 2009

Keywords:
DIOS
QuickMass™
Laser mass spectrometry
Metabolic profiling
Ionization mechanism

ABSTRACT

In the era of systems biology, new analytical platforms are under demand. Desorption/ionization on silicon mass spectrometry (DIOS-MS) is a promising high throughput laser mass spectrometry approach that has attracted a lot of attention, and has been commercialized. Another substrate material manufactured by physical method has also been made commercially available under the trade name of QuickMass™. These two commercial substrates, DIOS™ and QuickMass™, were investigated independently from the manufacturers and were characterized by a number of advanced surface techniques. This work determined (1) the correlation between the substrate physicochemical properties and their LDI activity, (2) the feasibility of metabolic profiling from complex biological matrices and (3) the laser desorption/ionization mechanism. The DIOS™ substrate was characterized with a thick nano-sized porous layer, a high surface concentration of fluorocarbon and silicon oxides and super-hydrophobicity. In contrast, the QuickMass™ substrate consisted of a non-porous germanium thin-film. The relatively high ionization efficiency obtained from the DIOS™ substrate was contributed to the fluorosilane manufacturing processes and its porous morphology. Despite the QuickMass™ substrate being less effective, it was noted that the use of germanium affords a self-cleaning mechanism and suppresses background interference of mass spectra. The suitability of DIOS™ substrates for metabolic profiling of complex biological matrices was demonstrated. DIOS mass spectra of human blood plasma, human urine and animal liver tissue extracts were produced. Suitable extraction methods were found to be important, but relatively simplified approaches were sufficient. Further investigations of the DIOS desorption/ionization mechanism were carried out. The previously proposed sub-surface state reaction could be a molten-solid interfacial state reaction of the substrate and this had a significant effect toward the protonation reaction of amines.

1. Introduction

The importance of metabolomics lies on the integrated systems biology, which seeks to understand the biological systems at the molecular level. Currently, metabolomics relies on chromatographic techniques coupled to mass spectrometry (MS) and proton nuclear magnetic resonance (NMR) spectroscopy approaches. However, these approaches either require a lengthy separation procedure before mass analysis or do not provide sufficient sensitivity. Furthermore, because of the heterogeneity of the metabolome, a single analytical approach cannot realistically cover the wide range classes of metabolites. Therefore, a new analytical platform, which is not throughput and sensitivity limited, is imperative for the development of metabolomics. Desorption electrospray ionization (DESI) [1–4], direct analysis in real time (DART) [5,6], plasma-assisted desorption/ionization (PADI) [7] and desorption/ionization on silicon (DIOS) [8] are examples of newly emerged MS approaches that allow rapid mass analysis of biological related small molecules.

Of all emerging MS technologies, DIOS appears to be a promising one. DIOS was first reported in 1999 [8]. The technique is closely related to matrix-assisted laser desorption/ionization (MALDI) but unlike the aforementioned emerging MS technologies, it does not require special interface or modification of the existing MALDI instruments. The development of DIOS aimed to provide a versatile platform for biomedical applications, principally in proteomics [9] and metabolomics [10]. The essence of the DIOS technique is the nanostructured porous silicon (PSi) substrate. PSi is a UV-absorbing semiconductor comprised of interconnected zero-dimensional nanocrystallites and one-dimensional nanowires produced through galvanostatic anodization, electrochemical or photochemical etching of crystalline silicon in the presence of HF [11]. Freshly etched PSi produced by chemical

* Present address: Clinical Sciences Research Institute, Warwick Medical School, University of Warwick, University Hospital, Clifford Bridge Road, Coventry, CV2 2DX, UK. Tel.: +44 24 7696 8634.
E-mail address: k.law@warwick.ac.uk.

1387-3806/$ – see front matter © 2009 Elsevier B.V. All rights reserved.
doi:10.1016/j.ijms.2009.12.006

anodization has a high surface concentration of Si–H. However, the Si–H surface slowly reacts with the ambient air [11,12]. Consequently, the chemical composition of a PSi surface and its properties evolve continuously with storage time. The growth of an oxide layer can significantly alter the PSi surface structure and generally leads to impairment of the DIOS activity [13]. One approach to address the instability of PSi is by chemical derivatization. In fact, the first generation DIOS substrates reported were either hydrogen- or phenethyl-terminated [11]. The subsequent development of the DIOS substrate adopted self-assembly of silanes on oxidized silicon surfaces to enhance stability or selectivity [14–18]. The DIOS technique had also since progressively enhanced overtime and recently re-emerged as nanostructure-initiator mass spectrometry (NIMS) [19–21].

Since the first report of DIOS-MS, several other matrix-free LDI substrates have been successfully developed and/or commercialized. The commercial products include DIOS™ target from Waters Corp., the QuickMass™ target from NanoHorizons, Inc. and Shimadzu, Corp and the NALDI™ chip from Nanosys, Inc. and Bruker Daltonics, Inc. The QuickMass™ targets consist of a nanometer-thick non-porous germanium layer deposited onto a supporting surface [22] such as glass microscope slide and standard stainless steel MALDI sample plates [23,24] and thus it is adaptable to wide range of target format. Prior to the deposition of the germanium layer, the surface may be coated with a hydrophobic layer to minimize spreading of sample droplet. Furthermore, the target is reportedly more reproducible and stable under ambient conditions than that produced by electrochemical etching. The manufacturing process is also relatively low cost, allowing the QuickMass™ targets a disposable platform for matrix-free high throughput laser mass spectrometry analysis of pharmaceutical products [25].

Nanostructured semiconductor substrates interfaced with the laser mass spectrometry have an immense potential in biomedical research. In particular, without the matrix dependence and interferences using the conventional organic matrix and the possibility of "chip-based" format, this approach permits a robust high throughput analytical approach for pharmaceutical products and biological related small molecules, in part addressing the challenges in metabolomics. Then again, despite intensive effort was paid to the investigation of the DIOS desorption/ionization mechanism [26–28], there is still a lack of experimental evidence and a vast gap of knowledge in this area.

In the previous report, various SALDI substrates were investigated [29]. Their surface morphology, chemical properties and suitability for complex biological matrix were discussed. Some of the factors that govern the SALDI activity were also revealed. In the second part of this study, focus was shifted to the commercial DIOS™ targets from Waters Corp. and the QuickMass™ targets from NanoHorizons Inc. These target substrates have been characterized and their LDI performance has been compared. The suitability for the analysis of various complex biological matrices is demonstrated. Experimental evidence that provides further insight of the DIOS desorption/ionization mechanism is revealed.

2. Experimental

2.1. Materials

Deionized water (18 MΩ) was generated by a USF Elga (Stoke-on-Trent, UK) Maxima water purification system. Gradient grade acetonitrile, HPLC grade methanol, isopropanol, formic acid, trifluoroacetic acid and phosphoric acid were purchased from Fisher (Loughborough, UK). Acetylcholine chloride, metoprolol tartrate, D-raffinose pentahydrate, reserpine, tetrabutylammonium hydrogen sulphate, tertahexylammonium bromide and cholic acid were purchased from Sigma–Aldrich and Fluka (Poole, UK). Atenolol was purchased from MP Biomedicals (Illkirch, France). Verapamil hydrochloride was purchased from Acros (Geel, Belgium).

2.2. Matrix-free LDI substrates

MassPREP™ DIOS™ targets and holders were purchased from Waters Corp. (Manchester, UK). The targets were shipped in a sealed argon-filled anti-electrostatic pouch and were stored in acetonitrile/isopropanol overnight in a Teflon bottle before use. This procedure, recommended by the manufacturer, greatly reduced organic residue originated from the packing material. QuickMass™ targets, with a special coating on a standard steel target, were obtained from NanoHorizons Inc. (Pennsylvania, US) and were shipped in a sealed container. The targets were used directly.

2.3. Surface imaging and topography analysis by scanning electron microscopy (SEM) and atomic force microscopy (AFM)

SEM analysis was carried out in high vacuum mode using a JEOL (Tokyo, Japan) JSM-6060LV SEM instrument. No gold coating was required. AFM investigation was carried out on a Dimension 3100 Scanning Probe Microscope (SPM) (Veeco, Santa Barbra, CA, USA) operated using a single laser beam under tapping-mode with an etched silicon probe tip (TESP). Acquired images were analysed using Image Metrology SPIP version 4.

2.4. Time-of-flight secondary ion mass spectrometry (ToF-SIMS)

SIMS analysis was performed with a TOF-SIMS IV instrument (ION-TOF GmbH, Münster, Germany). The instrument employed a 15 keV $^{69}Ga^+$ and 10 keV $^{133}Cs^+$ liquid metal ion gun (LMIG) with 10 kV post-acceleration and a single-stage reflectron analyser. The AC primary ion (PI) beam was pulsed at 10 kHz frequency using a current between from 1.06 and 1.17 pA for Ga^+ LMIG and 0.95 pA for Cs^+ LMIG, bombarding an area from $100 \times 100\,\mu m^2$ (for high mass resolution) to $500 \times 500\,\mu m^2$ (for high sensitivity). Both positive and negative ion spectra were acquired for each analysis area, with an ion dose of 5×10^{11} PI/cm^2 per polarity. Optical images were also taken. Calibration of the mass spectra in the positive detection mode was based on the following peaks, CH_2^+ (14.0157 amu), $C_2H_2^+$ (26.0157 amu), $C_3H_2^+$ (38.0157 amu), and $C_4H_3^+$ (51.0235 amu); and in negative detection mode on CH_2^- (14.0157 amu), C_2^- (24.0000 amu), C_3^- (36.0000 amu), C_4H^- (49.0078 amu). Data acquisition and post-processing analyses were performed using IonSpec Version 4.010.

2.5. X-ray photoelectron spectroscopy (XPS)

XPS was carried out on a Kratos AXIS Ultra (Kratos Analytical Ltd, Manchester, UK) instrument, using a monochromatic beam from an aluminium source run at 150 W. A take-off angle of 90° was used, and the samples were analysed with the charge neutralizer on. The survey and core level spectra were collected using a pass energy of 80 eV and 20 eV, respectively. Datafiles were collected using the instrument Vision 2 software and processed using CasaXPS version 2.3.1.2 with Kratos sensitivity factors. The spectra were corrected to position the C–C within the C 1s core level at a binding energy (BE) of 285.0 eV.

2.6. Water contact angle (WCA) measurement

WCA measurements were carried out using a KSV (Helsinki, Finland) CAM 200 system equipped with manual liquid dispenser, and a high-speed digital CCD fire-wire camera and LED based

stroboscope. Deionized water was used as the test liquid. The measurements were carried out at room temperature.

2.7. Biological samples preparation

Human blood plasma was obtained from blood bank. 100 μl of plasma was first crushed with 1000 μl of methanol. Plasma proteins were precipitated out. The solution was then vortexed for ~5 min and then pre-cooled to 4 °C and centrifuged for ~10 min. Clear supernatant was removed by a pipette. The extract was further diluted four or eight times using 1:1 ACN/H_2O. Further dilution was possible, but a higher concentration might suppress ion desorption. The serum extract was stored in −20 °C and was thawed at room temperature before analysis.

Human urine sample was collected from a male type II diabetic patient immediately before the extraction. 3 ml of urine was extracted by 5 ml of 9:1 diethyl ether/hexane. The aqueous layer was further extracted by 5 ml of 1:1 chloroform/butanol. The organic fractions were collected and the remaining aqueous fraction was discarded. The organic extracts were reduced volume to dryness by a centrifugal evaporator. The residue was reconstituted in 1:1 ACN/H_2O. The extract was stored in −20 °C and was thawed at room temperature before analysis.

Sprague Dawley® Rats (Charles River Laboratory, UK) were killed by stunning followed by decapitation and dissection. The rats were housed grouped four per cage and were free to access food (standard rat "chow"), and tap water *ad libitum*, with 12 h light/dark period. The rats' liver tissue was stored at −80 °C before extraction. The tissue sample was first washed with ample of deionized water to remove blood and blood clot residue and was then homogenized. About 4 g of homogenized liver tissue was extracted with isopropanol by sonication and was then centrifuged for 10 min. The supernatant was taken out and was further diluted 10 times using 1:1 ACN/H_2O. The extract was stored in −20 °C and was thawed at room temperature before analysis.

2.8. Laser mass spectrometry

Surface handling and analyte solution deposition were carried out in a laminar flow-hood to minimize atmospheric contamination. Analyte solution was deposited onto the target surface using a pipette. Analyte solution was prepared in 50% acetonitrile. Typically, 1 μl of solution was added on each sample spot and air-dried.

Mass spectra were acquired using a Micromass (Manchester, UK) M@LDI-TOF mass spectrometer operating in reflectron mode. Pulse voltage was 3500 V. Delay time extraction was 500 ns. Spectra were acquired at 5 Hz using a nitrogen laser (337 nm). Laser energy was attenuated by a motorised iris equipped for automated laser control. The laser energy was set to a constant value. Data acquisition and post-processing analyses were performed using MassLynx version 4.0. All data was acquired in positive ion mode.

Mass spectra were also acquired using a Micromass (Manchester, UK) Q-ToF Premier mass spectrometer, fitted with a MALDI ion source. The source housing incorporated a nitrogen laser (337 nm). The laser was operated at 20 Hz and was attenuated by a neutral density filter. The ion source housing also equipped with a capillary line and adjustable needle valve to introduce gas into the source to provide collisional cooling of the ion beam to the thermal levels in the hexapole ion guide and improve ion transferring efficiency. A travelling-wave stacked ring ion guide (SRIG) system propels ions to the collision cell and to the mass analyser [30]. Argon was used as collision gas. ToF mass analyser equipped with dual micro-channel plate MCP detector, operated in "V" (single focusing) or "W" (double focusing) mode. The MCP voltage was optimised, typical values were 1800 V to 2100 V. Mass resolution was ~8000 in V mode and ~14,000 in W mode. Data acquisition and post-processing analyses were performed using the MassLynx version 4.1.

2.9. Metabolite identification

Putative metabolites identification was carried out based on the exact mass (m/z) measurement using METLIN (http://metlin.scripps.edu/), Human Metabolome Project (http://redpoll.pharmacy.ualberta.ca/hmdb/HMDB/) databases, and Lipid Mass Spec. Predictor version 1.2 from Lipid Maps (http://www.lipidmaps.org/).

3. Results and discussion

3.1. Laser mass spectrometry investigation

On examining the LDI performance of the DIOS™ substrate against the QuickMass™ substrate, they both could generate good quality mass spectra and were able to detect a wide range of pharmaceutical compounds. Additionally, the mass spectra did not suffer interferences from matrix ion or surface contamination.

Fig. 1 shows representative positive ion DIOS mass spectra of atenolol, metoprolol, raffinose and acetylcholine. For the neutral pharmaceutical compounds that form protonated ion such as atenolol and metoprolol, molecular ion $[M+H]^+$ dominated the mass spectra and the sensitivity was mostly correlated positively to the proton affinity (PA) of the analyte [31,32]. However, it needs to stress that, because the activation energy of different class of compounds can vary considerably, it is the enthalpy of the reaction but not the PA ultimately determines such relationship or which compound tends to form a protonated ion [33]. On the other hand, saccharides were detected as salt adducts in positive mode. Pre-charged ions such as acetylcholine were detected was as M^+ ion and its fragment. Typical limit of detection for the pharmaceutical compounds, which have a high PA value, low ionization potential, or is UV-sensitive or pre-charged, was in the fmol range. Admixture of acidic modifier, such as formic acid, acetic acid, or TFA did not improve the ion yield. Admixture of phosphoric acid oxidized the surface and completely suppressed ion formation.

Fig. 2 shows representative positive ion mass spectra of verapamil, reserpine, tetrabutylammonium ion and tetrahexylammonium ion acquired from the QuickMass™ target. Molecular ion dominated the verapamil mass spectra and quasi-molecular ions $[M-H]^+$ dominated the reserpine mass spectra due to its low ionization energy. Although, mass spectra could be successfully acquired using the QuickMass™ targets, the sensitivity was relatively low. Ordinarily, for neutral compounds, a concentration of 0.1–0.5 mg/ml was required for the QuickMass™ substrate. Peptides, caffeine and complex mixtures did not ionize well either. This was consistent with the information provided by the manufacturer [23,24] and hence the target was marketed for pharmaceutical development. Nonetheless, pre-charged ions such as quaternary amines had a high sensitivity with the QuickMass™ substrate. This was because these molecules have already carried a positive charge and are desorbed from the surface by thermal reaction to overcome the electrostatic attraction of the counter ions and the desorption potential of the surface and require no energy input for the ionization step. For that reason using the ion intensity of a pre-charged ion as a quantifier to evaluate the LDI performance of a matrix-free LDI substrate could only provide information of its desorption efficiency, and not the desorption/ionization efficiency [34].

3.2. Surface morphology investigation by SEM and AFM

The surface imaging by SEM and AFM revealed the distinctive physical properties of the commercial targets in microscopic scale

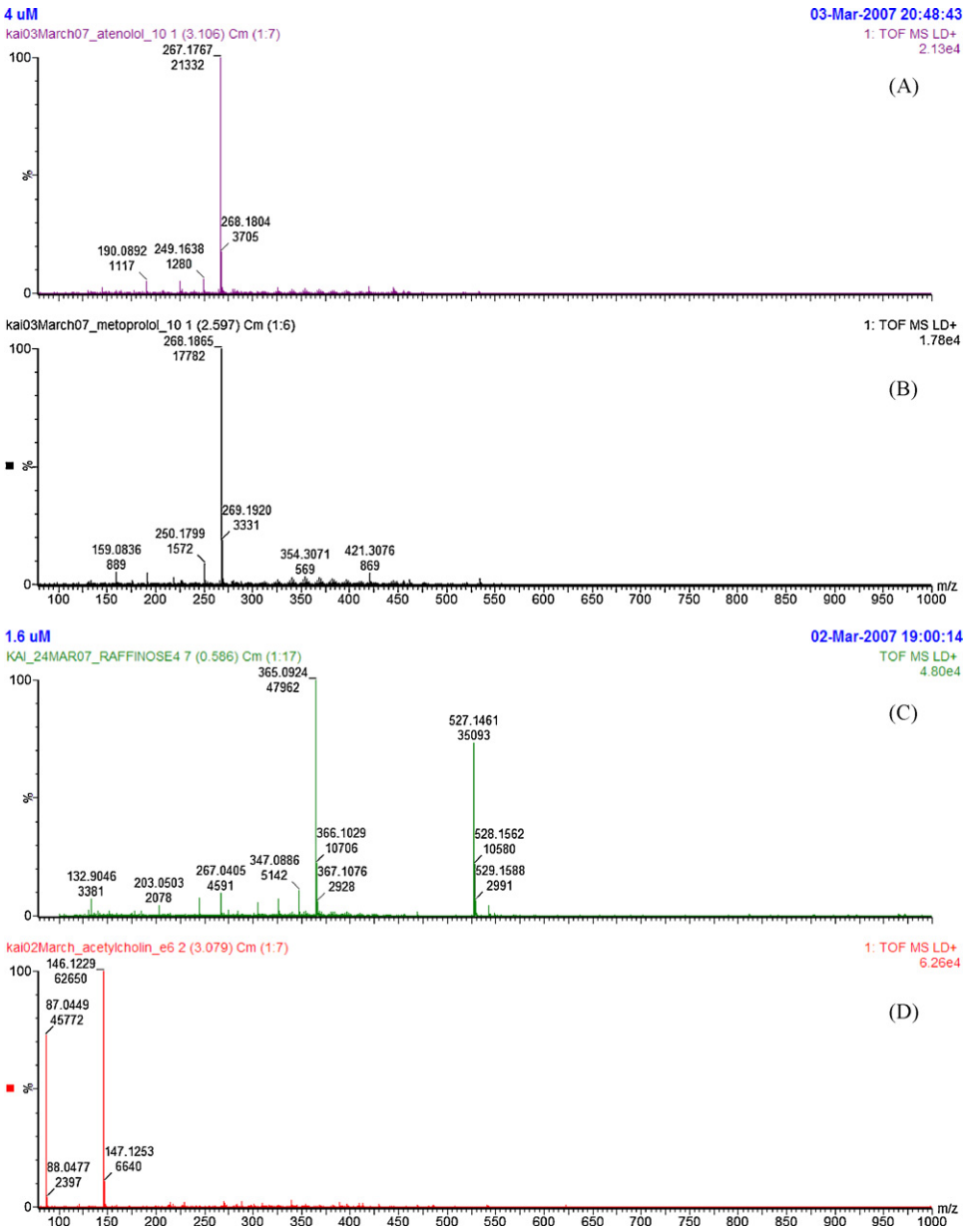

Fig. 1. Positive ion DIOS mass spectra of (A) atenolol, $[M+H]^+$ at m/z 267, (B) metoprolol, $[M+H]^+$ at m/z 267, (C) raffinose, $[M+Na]^+$ at m/z 527 and (D) acetylcholine chloride, M^+ at m/z 146. The spectra were acquired using a solution of 8 μM of atenolol, 4 μM of metoprolol, 1 mM of raffinose and 1.6 μM of acetylcholine chloride, respectively on the LDI-Q-ToF system.

that correlated strongly with their LDI performance and retention capability.

The SEM image (Fig. 3A) showed that the DIOS™ substrate has a thick porous layer and has pore openings varying from 20 to 200 nm. The AFM image (Fig. 3B) also indicated that a significant number of the pores are smaller than the size of the tip curvature (~30 nm) and appear as a convolution of the tip and pore entrance shapes. The results were consistent with the literature data reported previously [35].

In contrast, the SEM and AFM images (Fig. 3C and D) showed that the QuickMass™ substrates are non-porous. The surface is continuous but has voids parallel to the surface. It was noted that the surface morphology of the QuickMass™ substrates, does not share a similarity with the columnar/voids Si thin-film substrate produced by electron cyclotron resonance plasma-enhanced chemical vapor deposition (ECR-PECVD) described in [36–38]. According to the reference sources [39,40], the QuickMass™ substrate was prepared by physical vapor deposition (PVD) and this deposited thin-film replaced the columnar/voids film developed previously, because the columnar/voids film tended to have a high chemical background in the low mass region of the mass spectra, due to hydrocarbon contaminants adsorption. The targeted deposited thickness was 100 nm and was comparable with the vertical scale of AFM image obtained.

As shown by the surface morphology investigation, the DIOS™ substrate is porous whereas the QuickMass™ substrate is largely rough. The relatively low sensitivity of the QuickMass™ substrate appeared related to the low surface-to-volume ratio of the substrate and that led to lower ionization efficiency, compared to the porous and the high specific surface area DIOS™ substrate. However, since both substrates could generate good quality mass spectra, this further confirmed that the presence of pores is not strictly required for ion generation, but rather a factor affects the ion yield. An additional observation was that the ion signal dimin-

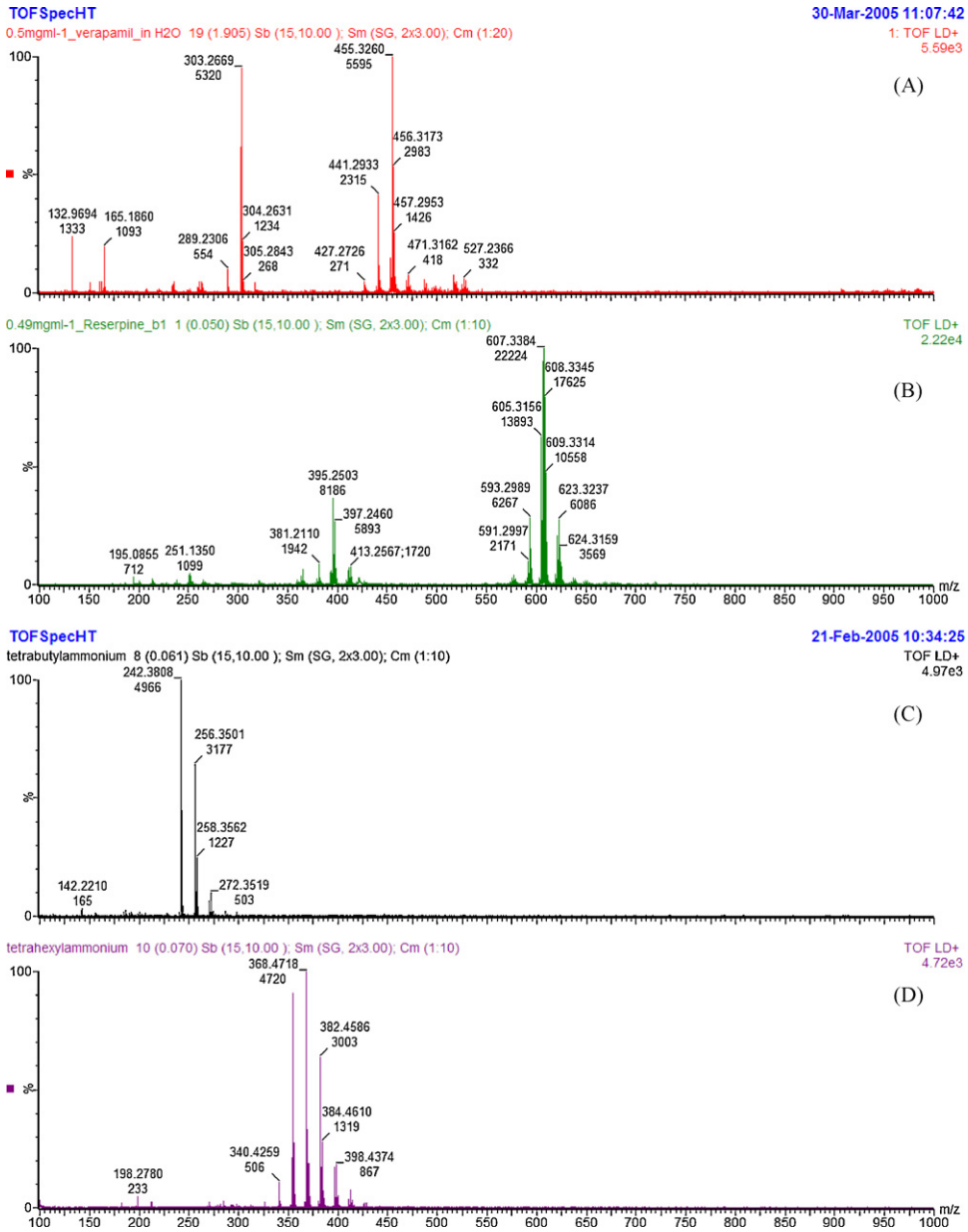

Fig. 2. Positive ion QuickMass™ mass spectra of (A) verapamil, $[M+H]^+$ at m/z 455, (B) reserpine, $[M-H]^+$ at m/z 607, (C) tetrabutylammonium hydrogen sulphate, M^+ at m/z 242 and (D) tetrahexylammonium bromide, M^+ at m/z 354. The spectra were acquired using solution of 0.5 mg/ml of verapamil and reserpine and 100 ng/ml of tetrabutylammonium hydrogen sulphate and tetrahexylammonium chloride, respectively on the LDI-ToF system. The quasi-molecular ions $[M-H]^+$ dominates the mass spectrum of reserpine due to relative its low ionization energy. A series of peaks, which differs by m/z 14 observed in the spectra of the quandary amines, was due to methylation reaction.

ished relatively rapidly on the QuickMass™ substrates. However, for the DIOS™ substrates, the ion signal lasted for many laser shots without relocation of the laser spot. This observation may relate to a desorption selectivity due to the surface morphology of the substrates. For the QuickMass™ substrate, the materials deposited on the surface were quickly consumed or vaporized by the heat induced by laser, whereas the pores on the DIOS™ substrate provide an additional function to retain the analyte in the confined space of the pores and to lower the neutral yield. Consequently, the proportion of ion yield relative to neutral yield is higher on the porous substrates. As a result, this led to the longevity of the signal and higher total ion intensity. Other possible reasons a thick porous structure tends to have a high performance included increased optical path length and UV absorbance, and encapsulation of air or solvent in the porous volume.

3.3. Chemical characterization by ToF-SIMS and XPS

The physical properties of the substrates only partly account for their LDI activity. The chemical characteristics of the substrates also play a pivotal role. To gain insight of the chemical properties of the substrates, the substrates were investigated by ToF-SIMS and XPS. ToF-SIMS was chosen to determine the surface molecular composition of the substrates because of its capability to determine the identity of the ions detected using accurate mass measurement. However, it was because the surface specificity of the SIMS technique, to gain a quantitative measurement of the surface elemental composition and the information on the bonding state of the substrates, XPS was also employed. Several important factors that affect the LDI activity are highlighted here.

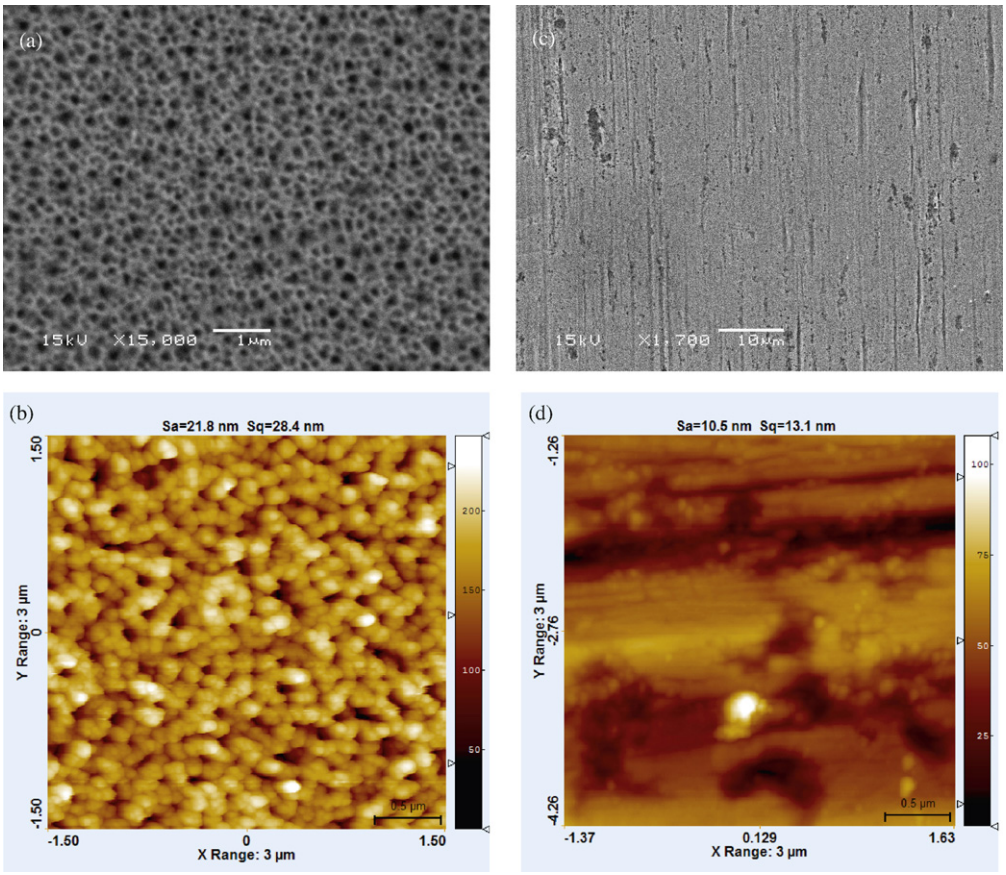

Fig. 3. SEM images and AFM images of (A and B) the DIOS™ substrates and (C and D) QuickMass™. Sa and Sq denote the roughness average and root mean square roughness of the image measured by AFM, respectively.

Representative SIMS spectra of the DIOS™ substrates are shown in supplementary materials, Fig. S-1. The SIMS spectra displayed typical characteristics of a silicon surface passivated with an oxide layer. The Si^+ ion dominates the positive spectrum and O^- and OH^- ions dominate the negative ion spectrum. In contrast, in the SIMS spectra of the QuickMass™ substrate (Fig. S-2) showed various germanium-related cluster ions (m/z 70–76) and germanium-oxide ions were also observed both in positive (m/z 85–93) and in negative (m/z 102–109) ion spectra, highlighting a significant difference in the substrate design and material used. The use of germanium in place of silicon is believed to afford a self-cleaning mechanism. For silicon, the thickness of oxides increases during the storage and that has been shown to be detrimental to the DIOS activity [41]. Germanium oxides, on the other hand, are unstable and are dissolvable by water. Once the sample solution is deposited onto the target, a fresh surface is exposed and thus unlike the DIOS™ target, the QuickMass™ target does not require inert gas sealed packaging and can be stored in air (covered) for a long time.

Representative XPS spectra of the DIOS™ substrate are shown in supplementary materials, Fig. S-3. Fluorine, oxygen, silicon and carbon dominated the survey spectra. Strikingly, the atomic concentration of fluorine was quantified as 18.4%. A few percent of fluorine is expected for freshly etched porous silicon surface and supposedly in the form of SiF_x (x = 1–3). On detailed inspection of the XPS spectra, it was apparent that the DIOS™ substrate had significant fluorocarbons assigned based on the C 1s core level spectrum that revealed CF_3, CF_2 and CO moieties (Fig. S-3C). The calculated surface concentration of fluorocarbons was approximately 15%. These indicated that the commercial DIOS™ targets were manufactured with fluorosilane derivatization. As discussed in the previous article [29], the fluorine on the surface is believed to have a practical role in increasing the water contact angle (see later) as well as acting as an electron withdrawing functionality from the oxygen increasing the acidity of the surface hydroxyl groups. These factors alter the electronic configuration of a silicon oxide surface and significantly enhance the ionization efficiency.

3.4. Water contact angle (WCA) measurements

The DIOS™ substrate has been recognized as hydrophobic based on the observation that aqueous droplets bead up on the surface [41]. As discussed in the previous article [29], the chemically functionalized SALDI substrates had different wettability, adsorption properties and SALDI activity than the unmodified substrates. Therefore, the commercial substrates were further characterized by WCA measurement.

The WCA of the DIOS™ substrate was approximately 132°. This was in contrast to the QuickMass™ substrates, which had a WCA of approximately 30°. Since the DIOS™ substrate has a significant concentration of fluorocarbon on the surface and unsurprisingly the surface was hydrophobic. However, the porous morphology of the substrate also has an important role in reducing the surface wettability.

A model to characterize the effect of the surface roughness on the wettability of a solid was first proposed by Wenzel [42]. This theory is only valid on the condition that the droplet has complete contact with the surface over their mutual interface. The condition does not meet for a porous hydrophobic surface. This is because the droplet has interfaces with the air being in the hollows of the pores and the droplet sits on the peaks of the surface feature. The droplet is therefore laid on a composite surface, composed of solid and air. This leads to a transition from the Wenzel to the Cassie/Baxter's sys-

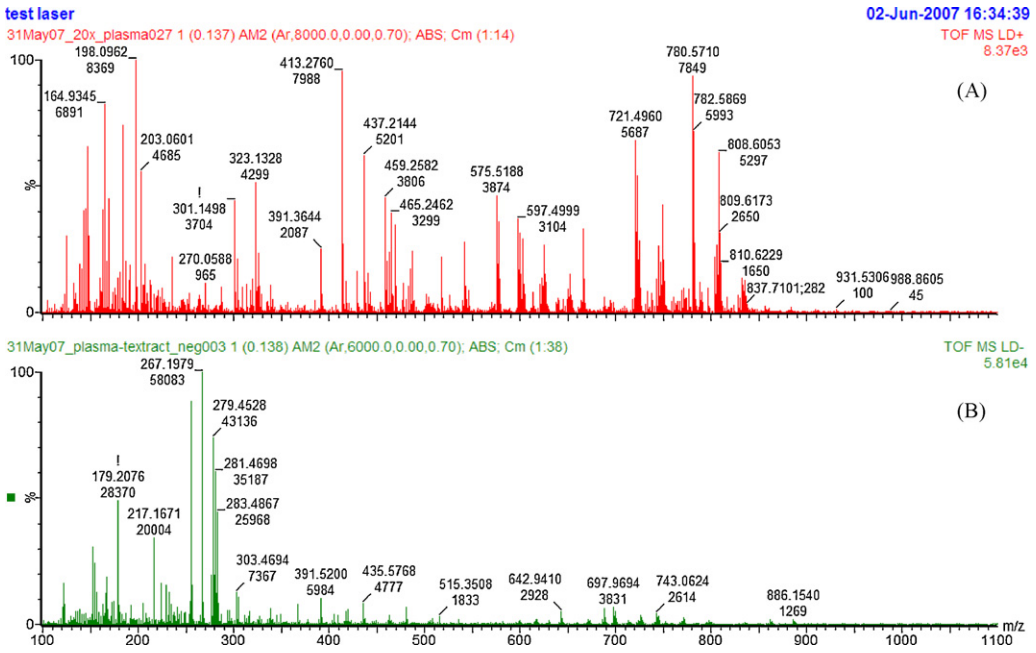

Fig. 4. (A) Positive and (B) negative ion DIOS mass spectra of human blood plasma extract. Mass spectra were acquired using the LDI-Q-ToF system and processed with automatic peak detection.

tem [43] and thus the DIOS™ surface exhibits super-hydrophobic properties. By using the Cassie's law, and taking $\theta_c = 132^\circ$, $\theta_1 = 109^\circ$, for the DIOS system, the calculated value of $f_1 = 0.49$. This indicates that only approximately 50% of the projected area was in contact with water.

The combined effects of fluorocarbon termination and the porous morphology of the DIOS™ substrate lead to reduction of the free surface energy and the cohesive force of the water droplet is thus greater than the adhesion force between the droplet and the surface. Qualitative test also showed that liquid droplet constituted of a high proportion of polar organic solvent (such as methanol and acetonitrile) was retained on the surface and there were no observable effect to the DIOS activity. This property has an important practical implication because some compounds such as phospholipids do not dissolve in water. Sample solution constituted of high proportion of polar organic solvent can therefore applied directly on the surface. The liquid confinement effect also ensures the enrichment of analyte molecules onto a small area contributing to the high LDI performance observed.

3.5. Complex biological matrices

In metabolomic studies, the experiments are usually conducted on biological fluids or tissue extracts, which contain a rich collection of metabolites. However, because of the complexity of a biological matrix and the ubiquitous salt content in biological samples produced interference, ion suppression and/or leads to adduct formation. A sample clean-up procedure was thus necessary to remove the salts and interfering materials and conserve the biological molecules of interest.

Sample preparation of blood plasma was relatively simple and only required precipitation of the albumin proteins. Alternatively, molecular weight cut-off filter could be used. The positive ion DIOS mass spectrum was information rich (Fig. 4). A number of lipids were located at the m/z 700–850 region. Sterol or fatty acid-like compounds were seen in the m/z 300–500 region. Glucose was detected as $[M+Na]^+$ at m/z 203. The spectrum also showed a peak set located at m/z 184.07 and 198.09 corresponds to $[C_5H_{15}NPO_4]^+$ and $[C_6H_{17}NPO_4]^+$, respectively and these ions were headgroup fragment ion of phosphatidylcholines. On the contrary, the anion formation was less favorable (see later) and the negative ion DIOS mass spectrum was not as information rich as the positive spectrum in comparison. The spectrum was dominated by a phosphate-containing contaminant located at m/z 267.

Although urine could be analysed directly without sample preparation (Fig. 5A and B), ion suppression was relatively strong. A sample preparation method that used diethyl ether/hexane and chloroform/butanol was adopted from [41]. The foundation for the two-step extraction approach had been discussed in [44] and demonstrated as being suitable for DIOS-MS. The method was slightly modified, such as the volume of urine used and the reconstitution of the dry residue. After sample preparation, there was a large increase in the number of ions generated both in the positive and negative ion spectra (Fig. 5C and D).

To assist the determination of the possible identities of the ions detected, metabolite database search was carried out. A list of detected positive ions derived from Fig. 5 of which the peak intensity above 5% of the base peak intensity threshold value was inputted to the METLIN metabolite database with a maximum of 5-ppm tolerance. The ions detected were assumed as molecular ions or sodium/potassium adducts of the metabolites present in the sample. The results are listed in the supplementary material table S-1. Although the search results were unconfirmed, the database matching reflected certain characteristics of the urine extract. For example, creatinine and creatine are known metabolites that present in high concentration in urine. Metformin is for the treatment of diabetes and concurs with the detection of glycation adduct (fructosamine) and the high intensity of glucose observed. [Note: another source of glycation adducts is diet] *N*-(2-hydroxyethyl)-nicotinamide and cotinine are metabolites of cigarette smoking in agreement with the life-style of the donor.

On examination of the negative spectrum of the urine extracts, there were four different ions distinctively detected in between mass range m/z 400–450 on the spectrum. While comparing the data with those available on the databases, *e.g.*, METLIN, it gave an impression that those were likely steroids/sterols, bile acids or related biomolecules, nevertheless it was difficult to determine the identity of those ions. With the aid of Q-ToF instrument, MS/MS

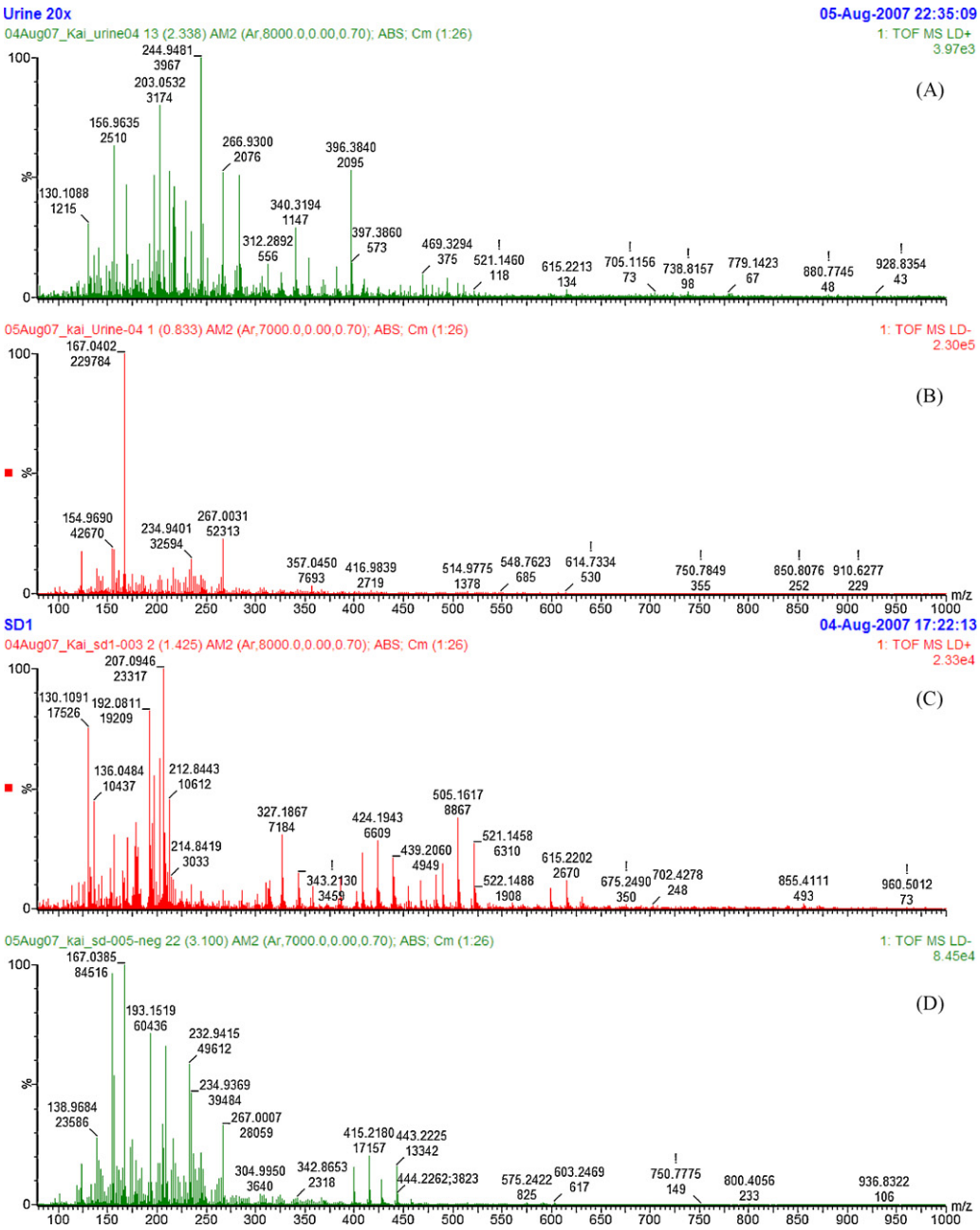

Fig. 5. (A) Positive and (B) negative ion DIOS mass spectra of a human urine sample. The sample was diluted 20 times with 50% ACN. (C) Positive and (D) negative ion DIOS mass spectra of the same human urine sample after sample preparation. Mass spectra were acquired using the LDI-Q-ToF system and processed with automatic peak detection.

analysis could be performed. The MS/MS spectra are shown in the supplementary material, Fig. S-4. Two major product ions of m/z 193 and 209 were detected. These fragment ions were also detected in the negative DIOS spectrum in Fig. 5. The product ions differed by m/z 16, or an oxygen atom, indicating that two of the precursor ions were possibly steroids and the other two were related sterols (deoxy-analogous).

Lipid metabolism and drug toxicity studies often involve liver tissue. To demonstrate that bimolecular analysis of tissue extract is also probable by DIOS-MS, DIOS mass spectra of rats' liver extract were acquired and the spectra are shown in Fig. 6. The positive ion spectra show a distinctive peak at m/z 184.07 and 198.09 corresponds to $[C_5H_{15}NPO_4]^+$ and $[C_6H_{17}NPO_4]^+$, and a number of peaks in the region m/z 600–900. As discussed earlier, these ions are most likely the headgroup fragment and sodium adducts of phosphatidylcholines. The negative ion spectra also show a number of distinct peaks in the same region.

A reviewer has pointed out that direct biofluid analysis could be explored further by taking the advantage of the surface affinity of the derivatized DIOS^{TM} substrate to capture the analyte of interest (the "Z-touch" approach) and minimize the sample preparation step [14,21]. In this method, an aqueous sample droplet is dragged over the surface using a pipette, leaving a residue on the surface. The aqueous droplet, along with inorganic salts and hydrophilic compounds, is then subsequently removed. While this method is promising, this method has not been fully exploited in this study. Firstly, it was because the method is more appropriate for the target that has a large sample spot diameter. The relatively small sample spot diameter of the commercial target presented a difficulty to permit the Z-touch approach practical. Secondly, it was an aim of

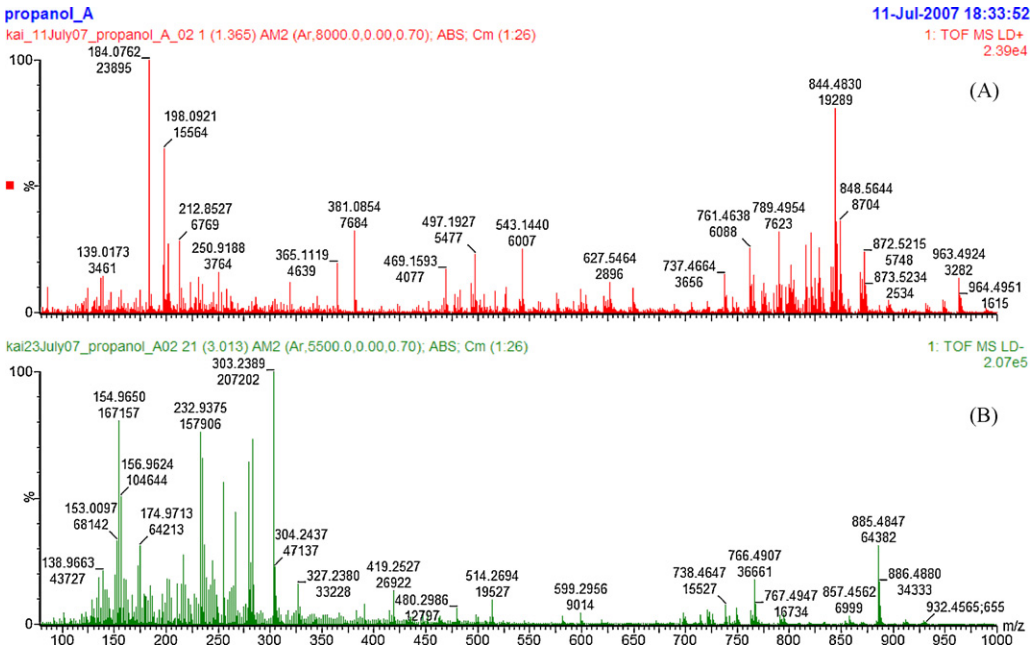

Fig. 6. (A) Positive and (B) negative ion DIOS mass spectra of rats' liver tissue extract. Mass spectra were acquired using the LDI-Q-ToF instrument and processed with automatic peak detection.

this study to prepare future cross-platform study. Effort was placed on determining suitable sample preparation methods compatible with both DIOS-MS and electrospray ionization, and a Q-ToF mass spectrometer capable of exchanging to-and-from an eletcrospary ion source and a MALDI ion source was used.

3.6. Investigation of the laser modification or ablation

Laser modification or ablation of the substrate is an important part of the ionization mechanism and the effects on the SALDI substrate has been investigated by ToF-SIMS ion mapping and XPS chemical imaging previously [29]. The effects of laser modification on the commercial DIOS^{TM} substrate are presented here. Fig. 7A shows the optical images of the DIOS^{TM} target before and after use for LDI mass spectrometry. A localized porous destruction occurred on the surface after the surface was used. In an extreme case, the surface was melted and recrystallized. A similar observation of a predominated hydride terminated DIOS substrate has been reported in [45]. Chemical transformation was thought to occur. However, ToF-SIMS investigation did not revealed any significant chemical change of the surface after the substrate had been used. This was explained by the fact that the DIOS^{TM} substrate used had already been chemically functionalized and passivated by an oxide layer.

Nevertheless, the detail of surface reconfiguration was observed by SEM (Fig. 7B). The SEM image on the left shows a sample well after LDI investigation. There were two distinct areas on the image. One was the area on a spiral burn-mark and the area outside this burn-mark. The spiral shape was due to the spiral stage movement, where the laser scanned different areas during data acquisition. This area showed a higher contrast relative to the area that had not been scanned or modified by laser. The high magnification image of area (a) revealed that there were two types of spherical particles. One of which had a higher contrast than the other type. This suggested that the chemical nature of these two types of particles was not identical. Conversely, this was less evidenced on the image of the non-modified region (b).

It is believed that the formation of the spherical particles was a consequence of surface melting or ablation due a localized high temperature induced by laser. Because of the low surface free energy of the surface, the molten silicon, like a drop of mercury, beaded up on the surface. Subsequent recrystallization of the molten silicon formed the spherical particles (the one with a high contrast). With increasing laser energy or prolonged laser bombardment, the rapid heating might have caused sublimation or vaporization of surface silicon, resulting in thinning the surface oxide layer. The particles could also be condensation of the ablated species (the one with low contrast). From these observations, it is very probable that it is the molten state of the silicon or the interfacial state of molten and solid state of silicon, which is important in the ion formation [46].

3.7. Detection characteristics

To gain further insight of the DIOS desorption/ionization mechanism, the ion intensity of the protonated ion and the fragment ions of verapamil as a function of the laser energy was plotted in Fig. 8A. The average ion intensity of the protonated ion increases exponentially from laser energy 100–180 and then drops from 190 to 220. The ion intensity then remains approximately a constant up to 300. Further increase of the laser energy beyond 300 leads to surface destruction. The mass spectra acquired have a very high chemical background (Fig. S-5) and the ion intensity of the protonated molecules and the fragment ion declines rapidly. The ion intensity of the fragment ions varies with the protonated ion and the ratio of protonated ion to the fragment ion is insensitive to the laser energy. A similar observation was reported in [26], but no reason was given. This was because of the filtering effect of the reflector. This situation happens when metastable decomposition occurs in between the ion source and the detector. The ions are lost by the reflector due to their change in kinetic energy and only the fragmentation in between the reflector and the detector can be detected.

Cholic acid is given as a further example here and it was detected in the negative ion mode (Fig. 8B). The ion intensity of the deprotonated ion of cholic acid also increases exponentially but a maximum is located at 250. The signal intensity decays from 250 onward. This is in contrast with the background ion located at m/z 267. The

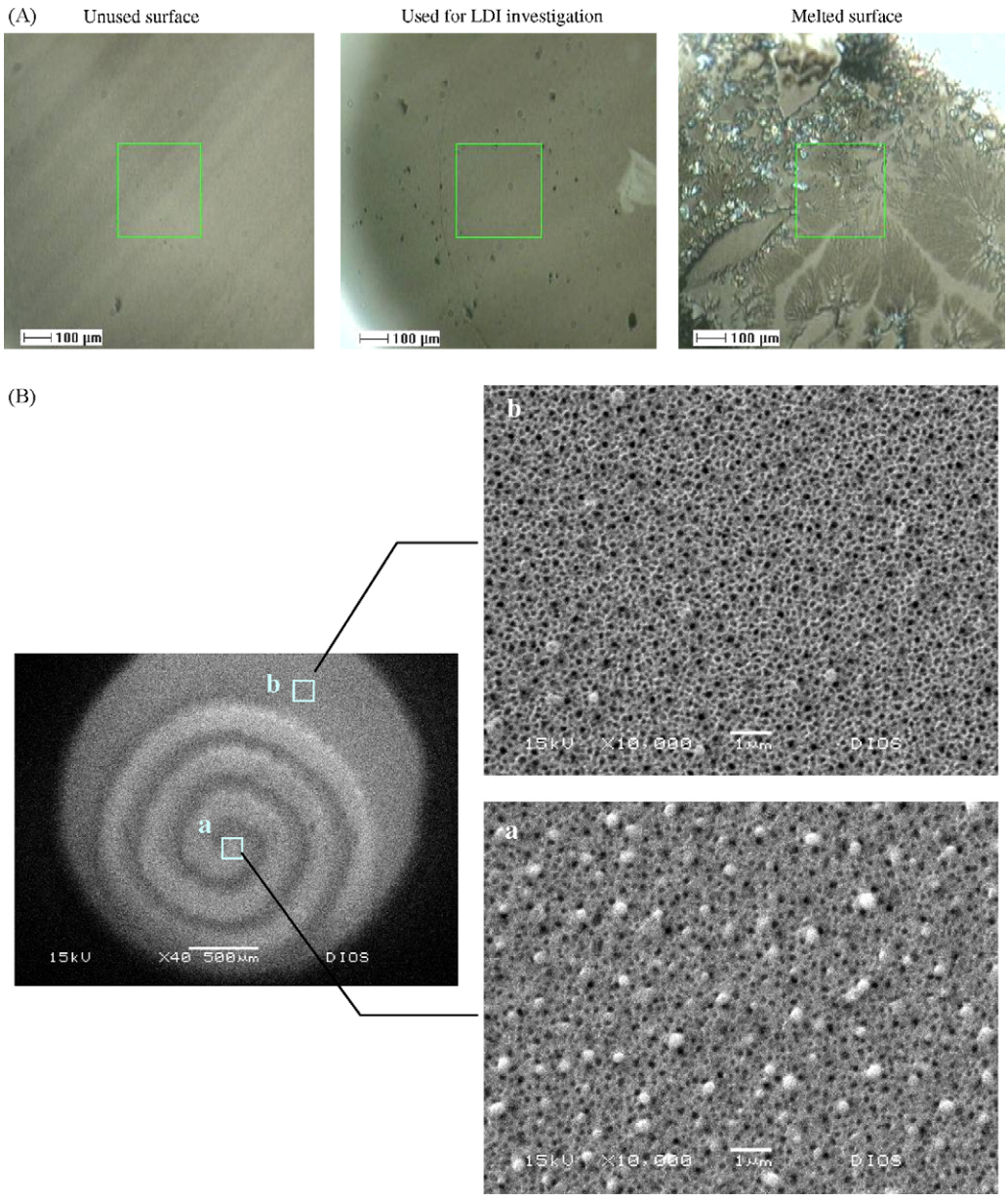

Fig. 7. (A) Optical image of a DIOS substrate that has not be used, used for LDI investigation, and damaged by laser. The LDI investigation was performed on the LDI-ToF system. (B) SEM images of a DIOS substrate after investigation. The surface had not been washed and stored in sealed container in freezer after use. The SEM image on the left shows a lower magnification of a sample well. The spiral shape laser "burn-mark" was formed because of spiral stage movement during data acquisition. Two areas were chosen with high magnification: (a) area that has not been modified by laser and (b) area that has been laser modified. The LDI investigation was performed on the LDI-Q-ToF system.

ion intensity of the background increases linearly with the laser energy and gradient starts to level off from 250. In other words, the signal-to-noise of the cholic acid decreases as the laser energy increases. Relative to verapamil, the ion yield of the deprotonated ion of cholic acid was one order lower despite the concentration used was 100 times higher. Apparently, the formation of negative ion was not "assisted" as much as the formation of positive ion. This was because of the chemical properties of the DIOS substrates that were optimized for positive ion formation. A silicon oxide surface is intrinsically acidic due to the chemical property of Si–OH surface termination. The acidity of the Si–OH moieties is further increased because of the electron withdrawing effect of surface fluorocarbon. Analyte deposited on the surface is thus surrounded in an acidic environment and this discriminates against the deprotonation of acidic compounds. It is apparent that increasing the surface basicity facilitates negative ion formation. As it has been recently demonstrated that only the silicon substrate that had either been derivatized with aminosilane or loaded with aminosilane initiator was effective for the desorption of negative ion of nucleotides [47].

Furthermore, it is speculated that small negatively charged molecular ions have innate instability when they are promoted to an excited state. This will be discussed further in the future report. Briefly, it was noted that a small negative charged molecule, which has a localized negative charge, has a strong tendency to recombine with a counter ion, or to form adduct or aggregate with alkali cation [48], and is consequently neutralized – estimated half-life is at least 1.5 orders lower in magnitude than that of positive ion. The compounds that can be effectively detected as deprotonated negative ion usually have a specific chemical property, such as an electronegative group that withdraws electron density from a localized negative charge, or an aromatic system that allows delocalization of negative charge [33,49]. These types of compounds

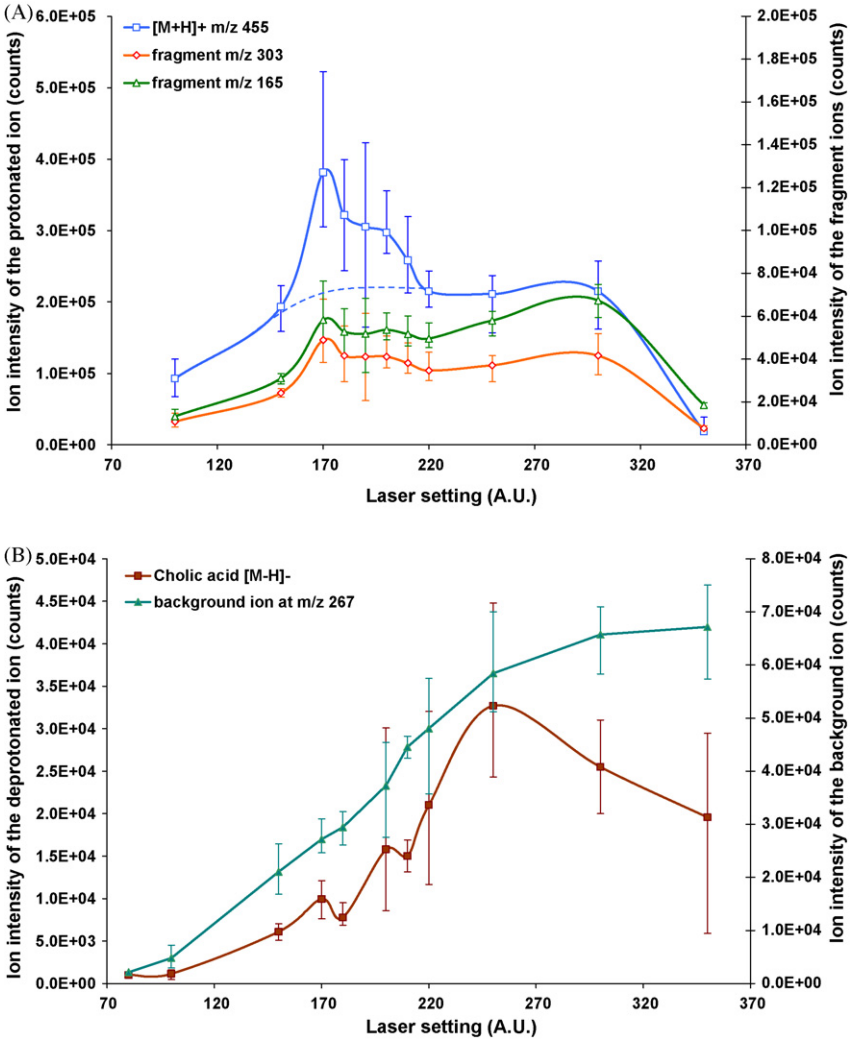

Fig. 8. Detection characteristics of (A) 500 ng/ml verapamil and (B) 0.1 mM cholic acid on the DIOS™ target. The secondary *y*-axis in (A) denotes the ion intensity of the fragment ions of verapamil and in (B) the background ion intensity located at *m*/*z* 267. The error bars denote the highest and the lowest value obtained. A dotted line is added in (A) to illustrate if the electronic processes were absent. Data was acquired using the LDI-Q-ToF system.

are not the common acidic metabolites that likely found in a high concentration in a healthy subject. This may further provide a reason that the negative ion biological DIOS mass spectra discussed above were less informative than the position ion mass spectra.

In addition, protonation reaction can be further assisted with electronic processes. The general tendency of increasing in ion yield before the surface destruction is believed due to the increasing thermal processes that promote the adsorbed molecules to an excited state and leads to ion formation. The differences between the detection characteristics of verapamil and cholic acid are believed due to the electronic processes of the molten state of the silicon. The electronic processes apparently work in a narrow range of laser energy at a rate that the energy input is just sufficient to melt the surface and forms an interface of molten and solid state of silicon nanocrystallite. This may explicate the first maximum obtained in Fig. 8A in between the laser energy 150 and 220. This process is clearly less significant in negative ion formation but has a significant effect in protonation reaction of amines and related compounds and is concurrent with the observations reported in [50]. The previously undefined "sub-surface state" of silicon therein could well be a molten-solid interfacial state. Increasing the laser energy further ablates the surface nanocrystallite and disrupts the electronic processes.

4. Conclusions

Despite ten years having passed since the DIOS-MS was first reported, the method has yet gained wide acceptance by the metabolomic community. A possible reason was that the information about the substrate characteristics that are effective for LDI-MS has been unavailable and the knowledge about its mechanism is still lacking. This study showed that the commercial DIOS™ substrate not only has a thick porous layer (over 250 nm) with majority of the pores in the meso- and macroporous range, it is also terminated with oxide moieties and passivated by a significant proportion of fluorocarbons. These surface properties or features of the DIOS™ substrate lead to a high LDI performance. On the other hand, the QuickMass™ substrate was revealed a non-porous germanium thin-film produced by PVD method which has reduced desorption/ionization yield compared with the DIOS™ substrate, but has the advantage of a surface chemistry which is resistant to surface contamination. It had also been shown that although the pores are not directly involved in ion formation, undoubtedly they are required for enhancing the ion yield and the porous substrates are the substrate of choice for biological mass spectrometry. It was demonstrated that the DIOS-MS has a relatively high versatility in analysing complex mixtures and metabolic profiles could be successfully acquired from biological matrices. The identifica-

tion of the metabolites was facilitated with the advanced mass spectrometry instrument capability, such as exact mass and tandem mass spectrometry. This expedited biomarker discovery and bought the DIOS-MS technique to the next level. Relative to the SALDI substrates described previously, the commercial substrates were readily to be used and immediately showed a higher LDI efficiency. Indeed, the mechanical strength as well as the radiation hardness of the substrate has a significant effect toward the ion formation and the quality of the mass spectra. A molten interface of the surface nanocrystallites was proposed here an important factor for the protonation reaction of amines and related compounds. Unlike the SALDI substrates described previously, the electronic and the thermal processes effect simultaneously, and in conjunction with other enhancements bought by the nano-porous structure and surface chemical properties, the DIOS™ substrate thus had the highest LDI efficiency in all the matrix-free substrates investigated. However, the assistance for the anion formation was still inadequate. Aminosilane derivatization was thought to be a method for enhancing the anion formation and investigation was underway.

Acknowledgements

This work was supported by RSC/EPSRC research funding. The author thanks Frank Rutten for assistance with the SIMS work, Emily Smith for assistance with the XPS work and the NanoHorizons Inc. and Waters Corp. for the QuickMass™ and DIOS™ sample and technical support. The author also thanks Dave Barrett and Morgan Alexander for their academic support during this study.

Appendix A. Supplementary data

Supplementary data associated with this article can be found, in the online version, at doi:10.1016/j.ijms.2009.12.006.

References

[1] Z. Takáts, J.M. Wiseman, B. Gologan, R.G. Cooks, Mass spectrometry sampling under ambient conditions with desorption electrospray ionization, Science 306 (2004) 471–473.
[2] R.G. Cooks, Z. Ouyang, Z. Takats, J.M. Wiseman, Ambient Mass Spectrom. Sci. 311 (2006) 1566–1570.
[3] Z. Takáts, J.M. Wiseman, R.G. Cooks, Ambient mass spectrometry using desorption electrospray ionization (DESI): instrumentation, mechanisms and applications in forensics, chemistry, and biology, J. Mass Spectrom. 40 (2005) 1261–1275.
[4] A. Venter, R.G. Cooks, Desorption electrospray ionization in a small pressure-tight enclosure, Anal. Chem. 79 (2007) 6398–6403.
[5] R.B. Cody, J.A. Laramee, H.D. Durst, Versatile new ion source for the analysis of materials in open air under ambient conditions, Anal. Chem. 77 (2005) 2297–2302.
[6] C. Petucci, J. Diffendal, D. Kaufman, B. Mekonnen, G. Terefenko, B. Musselman, Direct analysis in real time for reaction monitoring in drug discovery, Anal. Chem. 79 (2007) 5064–5070.
[7] L.V. Ratcliffe, F.J.M. Rutten, D.A. Barrett, T. Whitemore, D. Seymour, C. Greenwood, Y. Aranda-Gonzalvo, S. Robinson, M. McCoustra, Surface analysis under ambient conditions using plasma-assisted desorption/ionization mass spectrometry, Anal. Chem. 79 (2007) 6094–6101.
[8] J. Wei, J. Buriak, G. Siuzdak, Desorption/ionization mass spectrometry on porous silicon, Nature 399 (1999) 243–246.
[9] J.J. Thomas, Z. Shen, J.E. Crowell, M.G. Finn, G. Siuzdak, Desorption/ionization on silicon (DIOS): a diverse mass spectrometry platform for protein characterization, Proc. Natl. Acad. Sci. U.S.A. 98 (2001) 4932–4937.
[10] Z. Shen, E.P. Go, A. Gamez, J.V. Apon, V. Fokin, M. Greig, M. Ventura, J.E. Crowell, O. Blixt, J.C. Paulson, R. Stevens, M.G. Finn, G. Siuzdak, A mass spectrometry plate reader: monitoring enzyme and inhibitor activity with desorption/Ionization on silicon (DIOS) mass spectrometry, ChemBioChem 5 (2004) 921–927.
[11] M.P. Stewart, J.M. Buriak, Chemical and biological applications of porous silicon technology, Adv. Mater. 12 (2000) 859–869.
[12] J.M. Schmeltzer, J.M. Buriak, Recent developments in the chemistry and chemical applications of porous silicon, in: C.N.R. Rao, A. Müller, A.K. Cheetham (Eds.), The Chemistry of Nanomaterials: Synthesis, Properties and Applications, vol. 2, John Wiley and Sons, 2004, pp. 518–550.
[13] E.P. Go, J.V. Apon, W. Uritboonthai, B.J. Compton, E.S.P. Bouvier, M.G. Finn, Z. Shen, G. Siuzdak, Silyl chemical modification for desorption/ionization on silicon mass spectrometry (DIOS-MS): application to surface stability and analyte specificity, in: 52nd Annual Conference, ASMS, Nashville, TN, 2004.
[14] S.A. Trauger, E.P. Go, Z. Shen, J.V. Apon, B.J. Compton, E.S.P. Bouvier, M.G. Finn, G. Siuzdak, High sensitivity and analyte capture with desorption/ionization mass spectrometry on silylated porous silicon, Anal. Chem. 76 (2004) 4484–4489.
[15] E.P. Go, J.V. Apon, G. Luo, A. Saghatelian, R.H. Daniels, V. Sahi, R. Dubrow, B.F. Cravatt, A. Vertes, G. Siuzdak, Desorption/ionization on silicon nanowires, Anal. Chem. 77 (2005) 1641–1646.
[16] J.-C. Meng, C. Averbuj, W.G. Lewis, G. Siuzdak, M.G. Finn, Cleavable linkers for porous silicon-based mass spectrometry, Angew. Chem. Int. Ed. 43 (2004) 1255–1260.
[17] J.-C. Meng, G. Siuzdak, M.G. Finn, Affinity mass spectrometry from a tailored porous silicon surface, Chem. Commun. 21 (2004) 2108–2109.
[18] J.-C. Lee, C.-Y. Wu, J.V. Apon, G. Siuzdak, C.-H. Wong, Reactivity-based one-pot synthesis of the tumor-associated antigen N3 minor octasaccharide for the development of a photocleavable DIOS-MS sugar array, Angew. Chem. Int. Ed. 45 (2006) 2753–2757.
[19] T.R. Northen, O. Yanes, M.T. Northen, D. Marrinucci, W. Uritboonthai, J. Apon, S.L. Golledge, A. Nordstrom, G. Siuzdak, Clathrate nanostructures for mass spectrometry, Nature 449 (2007) 1033–1036.
[20] T.R. Northen, J.-C. Lee, L. Hoang, J. Raymond, D.-R. Hwang, S.M. Yannone, C.-H. Wong, G. Siuzdak, A nanostructure-initiator mass spectrometry-based enzyme activity assay, Proc. Natl. Acad. Sci. U.S.A. 105 (2008) 3678–3683.
[21] O. Yanes, H.-K. Woo, T.R. Northen, S.R. Oppenheimer, L. Shriver, J. Apon, M.N. Estrada, M.J. Potchoiba, R. Steenwyk, M. Manchester, G. Siuzdak, Nanostructure initiator mass spectrometry: tissue imaging and direct biofluid analysis, Anal. Chem. 81 (2009) 2969–2975.
[22] Product Introduction: QuickMass™ Disposable MALDI Plates High-Throughput Small-Molecule Analysis of Pharmaceutical Compounds, NanoHorizons Inc., 2005.
[23] R. Gallagher, P. Davey, I. Sinclair, R. Martin, M. Openshaw, A comparison between LCMS and Matrixless MALDI (LD) as rapid screening methods for high throughput analysis, in: 52nd Annual Conference, ASMS, Nashville, TN, 2004.
[24] R.L. Martin, P. Murray, Rapid characterization of small molecules using MS^n on a MALDI QIT TOF mass spectrometry, in: 52nd Annual Conference, ASMS, Nashville, TN, 2004.
[25] F. Xiang, J.D. Cuiffi, A.Y. Wang, D.J. Hayes, A new approach to small molecular analysis using matrix-less laser desorption and a hybrid mass spectrometer, potential for metabonomic applications, in: 53rd Annual Conference, ASMS, San Antonio, 2005.
[26] G. Luo, Y. Chen, G. Siuzdak, A. Vertes, Surface modification and laser pulse length effects on internal energy transfer in DIOS, J. Phys. Chem. B 109 (2005) 24450–24456.
[27] G. Luo, Y. Chen, H. Daniels, R. Dubrow, A. Vertes, Internal energy transfer in laser desorption/ionization from silicon nanowires, J. Phys. Chem. B 110 (2006) 13381–13386.
[28] Y. Chen, A. Vertes, Adjustable fragmentation in laser desorption/ionization from laser-induced silicon microcolumn arrays, Anal. Chem. 78 (2006) 5835–5844.
[29] K.P. Law, Surface assisted laser desorption/ionization mass spectrometry on nanostructured silicon substrates prepared by iodine-assisted etching, Int. J. Mass Spectrom. (2009), doi:10.1016/j.ijms.2009.12.003.
[30] K. Giles, S.D. Pringle, K.R. Worthington, D. Little, J.L. Wildgoose, R.H. Bateman, Applications of a travelling wave-based radio-frequency-only stacked ring ion guide, Rapid Commun. Mass Spectrom. 18 (2004) 2401–2414.
[31] P. Östman, J.M.H. Pakarinen, P. Vainiotalo, S. Franssila, R. Kostiainen, T. Kotiaho, Minimum proton affinity for efficient ionization with atmospheric pressure desorption/ionization on silicon mass spectrometry, Rapid Commun. Mass Spectrom. 20 (2006) 3669–3673.
[32] Y. Chen, H. Chen, A. Aleksandrov, T.M. Orlando, Roles of water, acidity, and surface morphology in surface-assisted laser desorption/ionization of amino acids, J. Phys. Chem. C 112 (2008) 6953–6960.
[33] Law, K., Matrix-free laser desorption/ionisation mass spectrometry on rough or porous semiconductor substrates: theory and applications, Ph.D. thesis, University of Nottingham, School of Pharmacy, 2008.
[34] Y. Xiao, S.T. Retterer, D.K. Thomas, J.-Y. Tao, L. He, Impacts of surface morphology on ion desorption and ionization in desorption ionization on porous silicon (DIOS) mass spectrometry, J. Phys. Chem. C 113 (2009) 3076–3083.
[35] G.M. Credo, H. Hewitson, C. Benevides, E.S.P. Bouvier, Development of a porous silicon product for small molecule mass spectrometry, Mat. Res. Soc. Symp. Proc. 808 (2004) 471–476.
[36] A.K. Kalkan, S. Bae, H. Li, D.J. Hayes, S.J. Fonash, Nanocrystalline Si thin films with arrayed void-column network deposited by high density plasma, J. Appl. Phys. 88 (2000) 555–561.
[37] J.D. Cuiffi, D.J. Hayes, S.J. Fonash, K.N. Brown, A.D. Jones, Desorption-ionization mass spectrometry using deposited nanostructured silicon films, Anal. Chem. 73 (2001) 1292–1295.
[38] A.K. Kalkan, M.R. Henry, H. Li, J.D. Cuiffi, D.J. Hayes, C. Palmer, S.J. Fonash, Biomedical/analytical applications of deposited nanostructured Si films, Nanotechnology 16 (2005) 1383–1391.
[39] Hayes, D.J., Micrototal analysis system for enzymatic drug metabolism and analysis, Ph.D. thesis, The Pennsylvania State University, Department of Engineering Science and Mechanics, 2004.

[40] Fonash, S.J., Bae, S., Hayes, D.J., Cuiffi, J., Deposited thin films and their use in detection, attachment, and bio-medical applications, US Patent 2002, US 20020048531.
[41] Z. Shen, J.J. Thomas, C. Averbuj, K.M. Broo, M. Engelhard, J.E. Crowell, M.G. Finn, G. Siuzdak, Porous silicon as a versatile platform for laser desorption/ionization mass spectrometry, Anal. Chem. 73 (2001) 612–619.
[42] R.N. Wenzel, Resistance of solid surfaces to wetting by water, J. Ind. Eng. Chem. 28 (1936) 988–994.
[43] A.B.D. Cassie, S. Baxter, Wettability of porous surfaces, Trans. Faraday Soc. 40 (1944) 546–551.
[44] K. Chatman, T. Hollenbeck, L. Hagey, M. Vallee, R. Purdy, F. Weiss, G. Siuzdak, Nanoelectrospray mass spectrometry and precursor ion monitoring for quantitative steroid analysis and attomole sensitivity, Anal. Chem. 71 (1999) 2358–2363.
[45] T.R. Northen, H.K. Woo, M.T. Northen, A. Nordström, W. Uritboonthail, K.L. Turner, G. Siuzdak, High surface area of porous silicon drives desorption of intact molecules, J. Am. Chem. Soc. 18 (2007) 1945–1949.
[46] Y. Wada, T. Yanagishita, H. Masuda, Ordered porous alumina geometries and surface metals for surface-assisted laser desorption/ionization of biomolecules: possible mechanistic implications of metal surface melting, Anal. Chem. 79 (2007) 9122–9127.
[47] A. Amantonico, L. Flamigni, R. Glaus, R. Zenobi, Negative mode nanostructure-initiator mass spectrometry for detection of phosphorylated metabolites, Metabolomics 5 (2009) 346–353.
[48] N. Budimir, J.-C. Blais, F. Fournier, J.-C. Tabet, The use of desorption/ionization on porous silicon mass spectrometry for the detection of negative ions for fatty acids, Rapid Commun. Mass Spectrom. 20 (2006) 680–684.
[49] H. Kawasaki, Y. Shimomae, T. Watanabe, R. Arakawa, Desorption/ionization on porous silicon mass spectrometry (DIOS-MS) of perfluorooctane sulfonate (PFOS), Colloid Surf. A 347 (2009) 220–224.
[50] S. Alimpiev, A. Grechnikov, J. Sunner, V. Karavanskii, Y. Simanovsky, S. Zhabin, S. Nikiforov, On the role of defects and surface chemistry for surface-assisted laser desorption ionization from silicon, J. Chem. Phys. 128 (2008) 014711–014719.